

STATIC AND DYNAMIC WIND-TUNNEL TESTING OF A TRANSPORT AIRCRAFT MODEL IN-STALL AND POST-STALL FLIGHT REGIMES

Dominique Farcy[1], Simon Prince[2], Mushfiqul Alam[2], Geoffrey Tanguy[1], Nicolas Vauchel[1] & Anderson Proenca[2]

[1] Univ. Lille, CNRS, ONERA, Arts et Metiers Institute of Technology, Centrale Lille Institut, UMR 9014 - LMFL - Laboratoire de Mécanique des Fluides de Lille - Kampé de Fériet, F-59000 Lille, France

dominique.farcy@onera.fr, geoffrey.tanguy@onera.fr, nicolas.vauchel@onera.fr

tel : +33 3 20 49 69 22 / 54 / 71

[2] Centre for Aeronautics Propulsion and Power, Faculty of Engineering and Applied Science (FEAS), Cranfield University, United Kingdom
simon.prince@cranfield.ac.uk, Mushfiqul.Alam@cranfield.ac.uk, A.Proenca@cranfield.ac.uk

Abstract

This paper presents static and dynamic wind-tunnel tests conducted on a 1/14-scale model of a transport aircraft to support flight-dynamic modelling in-stall and post-stall regimes. Experiments were performed at Cranfield University's 2.4 x 1.8m wind tunnel facility and ONERA's SV4 vertical wind tunnel using complementary test techniques. Results highlight hysteresis effects in static stall characteristics and demonstrate the dominant influence of rotation rate about the velocity axis on stall departure tendencies.

Keywords: wind-tunnel testing, stall and post-stall aerodynamics, dynamic aerodynamic effects, stability and control derivatives, flight dynamics

1. Introduction

The prediction of aircraft flight dynamics in low-speed regimes, including high-lift configurations and high angles of attack, requires aerodynamic models capable of representing forces and moments over an extended operating envelope. Such models must capture not only static non-linearities associated with stall, but also dynamic effects, particularly those arising from rotational motion about the velocity vector and unsteady aerodynamic phenomena such as dynamic stall. Accurate modelling in these regimes is essential for the prediction of hazardous flight conditions, the extension of aerodynamic models used in training and engineering simulators, and, more broadly, for the improvement of flight safety.

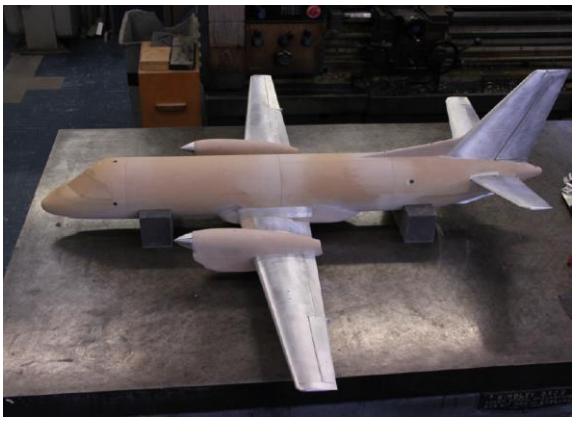
In this context, a collaborative research program has been established between Cranfield University and ONERA to develop and validate flight-dynamic models applicable to transport aircraft operating near and beyond stall. An asset owned and operated by Cranfield University is the flying laboratory aircraft G-NFLB, a 34-seater Saab 340B twin turboprop commuter airliner, shown in Figure 1. The aircraft is operated by a department of the university, the National Flying Laboratory Centre (NFLC). The Saab 340B has been selected as a representative regional turboprop configuration for this study.

https://doi.org/10.71945/icas2026_0203



Figure 1 - Cranfield University's Saab 340B twin turboprop (photo credit: Keith Wilson/SFB Photographic).

Dedicated flight-test data have been exploited for aerodynamic model identification, alongside complementary approaches based on numerical methods, including vortex-lattice modelling and DATCOM-based estimations [1–3]. In parallel, using using a 1/14th scaled model of the Saab 340B (see Figure 2a) wind-tunnel experiments were conducted at Cranfield's 8x6 feet low-speed wind-tunnel (see Figure 2b), with primary emphasis on the longitudinal aerodynamic behaviour up to stall.



(a) 1/14th scaled model of the Saab 340B aircraft operated at Cranfield.



(b) Test section of Cranfield's 2.4 x 1.8m low speed wind-tunnel.

Figure 2 - Wind-tunnel testing at Cranfield University.



Figure 3 - Model on rotary balance in SV4 ONERA Wind Tunnel.

https://doi.org/10.71945/icas2026_0203

To extend the aerodynamic database into regimes associated with stall departure and incipient spin, additional wind-tunnel testing was performed at ONERA. Experiments were conducted in the SV4 vertical wind tunnel, shown in Figure 3, using a rotary balance, employing the same reduced-scale model. Static and dynamic tests, including coning and oscillatory coning motions, were carried out to measure aerodynamic forces and moments under conditions representative of post-stall flight. Particular attention was given to the influence of rotation rate about the velocity axis, identified as a governing parameter in determining the tendency towards departure.
The contribution of this paper is the presentation of a combined static and dynamic wind-tunnel dataset for a regional turboprop transport aircraft model, covering pre-stall, stall, and post-stall conditions. The data demonstrate the limitations of static aerodynamic modelling alone and show the need to include sideslip, control-surface deflection, and rotation-rate effects when modelling departure-prone flight regimes.

2. Experimental Setups

2.1 Static Tests at Cranfield University

Wind-tunnel tests were conducted in the **Cranfield 8×6 low-speed wind tunnel** at **Cranfield University**, a closed-return facility capable of freestream velocities up to 50 m s^{-1}. The tunnel provides a controlled environment for measuring aerodynamic forces and moments relevant to flight-dynamic modelling. A **1:14 scale model of the Saab 340B** was tested. The model was geometrically representative of the full-scale aircraft and included adjustable primary control surfaces, with the exception of trim tabs. The model was unpowered; propellers and landing gear were not installed, although the nacelles were retained.
The model was mounted inverted in the test section using two wing struts and a single tail strut. The wing struts were attached at approximately 45% chord, while the tail strut controlled the model incidence angle and was connected to an overhead six-component Aerotech balance. The balance measured the three aerodynamic forces and three moments acting on the model. The support system was mounted on the tunnel ceiling turntable, allowing sideslip angle to be introduced where required. Aerodynamic moments were measured with respect to the virtual centre of the balance, located at the centre of the test section.
Boundary-layer transition was fixed on the main aerodynamic surfaces to improve repeatability and enable meaningful comparison with other experimental and flight-test datasets. Transition strips of 0.2 mm height and 5 mm width were applied to the wing, horizontal tail, vertical tail, fuselage nose, and nacelles. Their locations were selected using representative full-scale Reynolds-number considerations, with the lifting surfaces treated approximately as flat plates for transition estimation. Additional tuft-flow visualisation was also performed on the wing, horizontal tail, and rudder surfaces to support qualitative interpretation of the force and moment measurements, particularly in the stall regime.

2.2 Static and Rotary Tests at ONERA

2.2.1 Rotary balance description

Tests at ONERA were conducted in the SV4 wind tunnel located on the ONERA site at Lille, the test section has a diameter of 4 m and flow velocity can be up to 50 m/s.

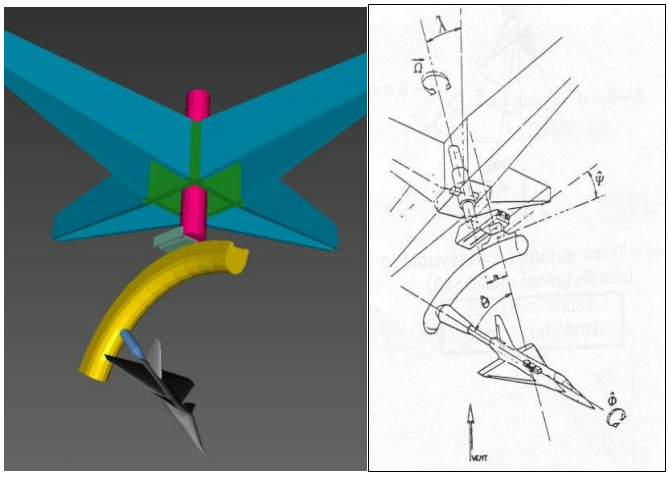


Figure 4 - Artist view of the rotary balance and definition of the angles

The main degrees of freedom of the rotary balance are the following (see Figure 4):
ϕ: lateral attitude of the model. It is the rotation around the longitudinal axis of the sting. This motion is motorized, and actuated without wind or rotation;

θ: longitudinal attitude of the model. Theta is due to a rotation around a horizontal axis going through the centre of the balance, and is obtained by the displacement of the (yellow) curved strut. It corresponds to the angle between the longitudinal axis of the sting and the direction of the rotation vector Ω.

ψ: heading angle of the model, (continuously variable during a rotation).

Ω: continuous rotation of the apparatus. The rotation can be constant during a test, or can follow a specific law of variation (coning motion).

λ: tilt angle between the rotary axis and the vertical axis. This motion is provided by an electrical motor. This motion is used to obtain quasi static polars. An oscillatory coning motion is obtained with the combination of non zero values of λ and Ω

The table below shows the main specifications of these degrees of freedom:

Table 1. Main specifications of the rotary-balance degrees of freedom.

Angle	Description	Range	Maximum rate
ϕ	lateral attitude of the model	-180° to 180°	$\lvert d\phi/dt \rvert$ = 2°/s
θ	longitudinal attitude of the model	0° to 45°	$\lvert d\theta/dt \rvert$ = 0.3°/s
ψ	heading angle of the model	0° to 360°	$\lvert d\Psi/dt \rvert$ = 700°/s
Ω	continuous rotation of the apparatus	-700°/s to 700°/s	$\lvert d\Omega/dt \rvert$= 50°/s^2
λ	tilt angle between the rotary axis and the vertical axis	0° to 30°	$\lvert d\lambda/dt \rvert$ = 1°/s

All degrees of freedom are motorised. The λ variation leads to quasi-static sweep in (α, β) domain (polar test). Only one degree of freedom actuated at the same time.

In the aim to identify classical static and dynamic stability aerodynamic coefficients, the following three types of test are carried out:
Quasi static sweeps in angle of attack at given sideslip angles. The angle of attack angle varied at about 1°/s.

Coning tests. During such tests, angle of attack and sideslip angle are fixed with the value of the θ and ϕ angles. The rotation rate is slowly varying between 0, maximum value (700 °/s) and minimum value (–700°/s). The rotation acceleration is 50°/s^2, the test is considered as a quasi steady test (no unsteady effect expected).

Oscillatory coning tests. These tests differ from the last tests in the fact that the lambda angle is set to a non zero value, which induces periodic variations of the angle of attack and the sideslip angles during one turn. The amplitude of those variations is equal to lambda. This angle is chosen relatively small (generally 5°) when the objective is to identify the dynamic stability derivatives (linearity assumption). Characterization of unsteady aerodynamics at high angle of attack including the dynamic stall phenomenon can be done by using larger values of lambda.

With a rear sting attachment the reachable range of angle of attack for static tests is [-75 +75°] and for coning test is [-45° 45°], complementary tests with dorsal or ventral attachment can allow higher angles of attack (negative or positive) up to +-90°, this is done in particular for the prediction of the spin (moderate to flat spin) (right or inverted) especially for combat aircraft or light airplanes, as described for example in [4].

2.2.2 Model setup and test plan

The 1:14 scale model is mounted on the rotary balance by the means of a cranked sting, which goes through the ventral rear part of the fuselage. An internal 6-components dynamometer (“balance”) is located inside the model. On a kinematical point of view this mounting is similar to rear-sting mounting. As objective is mainly focused on stall region, only positive values of angle of attack are considered. Static tests are performed at angles of attack in [0 50°] domain and angle of sideslip in [0 30°].

en done for angle of attack between 0 and 40° and sideslip angle between 0 and 15° in order to cover all the normal flight domain and also the stall and post-stall regime. Each coning test consists in a variation of rotation rate between -500 to +500 °/s, which allows to capture all eventual non-linearities. Various configurations of control surfaces settings were tested.

It must be noted that the model is equipped with transition devices on all lifting surfaces as it has been tested in Cranfield wind tunnel.

The parameter of similitude for transposition between reduced and full scale when dynamic aspects are considered is the reduced rate of rotation $\Omega b/2V$ where b is the total span of the model. In order to maximize this parameter, we have to do a compromise between high rate of rotation and low value of velocity. High rate of rotation induces high inertial effects, so the balance may be overloaded. Low value of velocity may lead to low aerodynamic effects, which can be difficult to measure; moreover, aerodynamics may change a lot with velocity due to potential Reynolds effects.

Even though rate of rotation can be up to +700°/s on the rotary balance, measurements on rotary balance were performed with rotation rate about velocity axis from -500 to +500°/s (main limitation is related to the weight of the model, 30 kg and the choice of a high-sensitivity balance) and at a velocity V=35 m/s. The rotary-test conditions (Ωmax=500°/s and V=35 m/s) were selected in order to get values of rate of rotation which seems realistic for full-scale aircraft. This leads to a maximal reduced value of rotation rate $\Omega^* = \Omega.b/2V=0.19$. We may transpose that to full scale aircraft, and consider the extreme case of fully developed spin (vertical trajectory), where weight is balanced by aerodynamic drag, which leads with the chosen aircraft to a velocity of about 60 m/s. In these conditions the maximal rate of rotation during the tests $\Omega^*=0.19$ would correspond to a rate of rotation of 60°/s on full scale aircraft (or 6s per turn of established spin).

Oscillatory coning test have also been carried out, in this case the axis of rotation is tilted relative to flow axis, which allows dynamic variations of angles of attack and sideslip, and therefore identification of dynamic effects, for example dynamic stall.

Analog measures coming from the model, the handling arm and the tunnel are low-pass filtered), sampled, digitalized and acquired at a frequency of 250Hz. Data are averaged according to discrete values of the time varying parameter of the test (longitudinal attitude of the model, rate of rotation or

time).
Aerodynamic coefficients are calculated from the difference between wind-on and wind-off balance measures, for a given configuration.

3. Results and discussion

Main results will be relative to:
- Static effects due to angles of attack and sideslip, at neutral deflections of control surfaces
- Effects of control surfaces
- Effect of rotation about velocity axis (coning tests)
- Effect of rapid change of angle of attack and sideslip (oscillatory coning tests).

Aerodynamic coefficients are calculated with the following choices for references:
- reference area: S=0.2133 m^2
- reference span: b=1.531 m (for definition of reduced rate of rotation)
- reference chord: c=mac=0.1486 m (length of reference for coefficients of moment)

The reference point for moments is located at 28.3 % of mean aerodynamic chord (mac). That corresponds to a point on the longitudinal axis of the model, at a distance of 0.612 m to the nose. All results in the paper are expressed at this point.
Classical choices are taken for definition of wind axes and body axes frame. Results concerning the moments are presented in body axes (Cl, Cm and Cn aerodynamic coefficients), with therefore the classical sign convention: Cl>0: right wing downwards effect , Cm>0: pitch-up effect and Cn>0: nose to the right effect. Aerodynamic forces coefficients are expressed in wind axes, with the standard choices of sign and notations (coefficient of drag: CD, coefficient of lift: CL) or in body axes (Cx, Cy, Cz).

For rotary effects, Ω is positive according to right-hand convention (Ω is positive when right wing is going downward) and results are plotted in function of reduced rotation rate $\Omega^*=\Omega b/2V$ where b is the total span of the model.

3.1 Static effects

3.1.1 Effect of velocity

Tests at Cranfield have shown a strong dependence to flow velocity (on a reduced test range, between 30 and 40 m/s) mainly in the stall region. On the rotary balance slow sweeps in angle of attack between 0 to 30° have been done for velocity between 10 to 50 m/s and confirm this result (Figure *5*). This strong dependence of the static stall characteristics on test velocity, with the stall angle increasing substantially between 10 m/s and 50 m/s, is a classical Reynolds-number sensitivity for low-speed wind-tunnel tests on model-scale (performed tests correspond to Reynolds number based on the mac between 10^5 and 5.10^5).
Stall angle increases quite rapidly with velocity, from a value of 9° at V=10 m/s to a value of 17° at V=50 m/s. For velocities higher than 25 m/s there exists different regions before the stall, in function of the slope of the lift force coefficient. In particular at V=50 m/s a limited region exists where stagnation of the lift slope is visible (around alpha=11°). For higher angles lift continues to increase up to maximal lift (1.35) attained at alpha=17°.

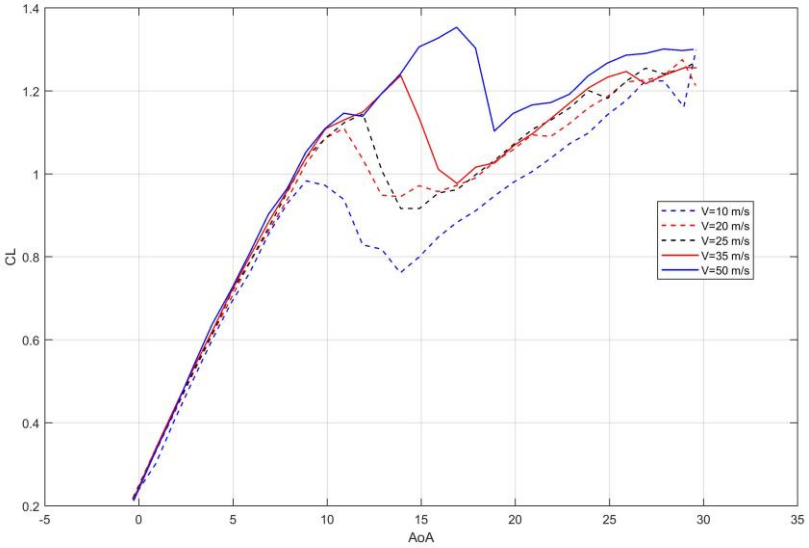


Figure 5 - Lift coefficient for V=10 to 50 m/s (beta=0).

3.1.2 Hysteresis effect

Comparisons between static wind-tunnel measurements obtained at ONERA and Cranfield University demonstrate a clear dependence of the aerodynamic response in the stall regime on the sense of angle-of-attack variation, highlighting the presence of hysteresis effects (see Figure 6). These effects are particularly pronounced in the post-stall region and underline the importance of path-dependent aerodynamic modelling.

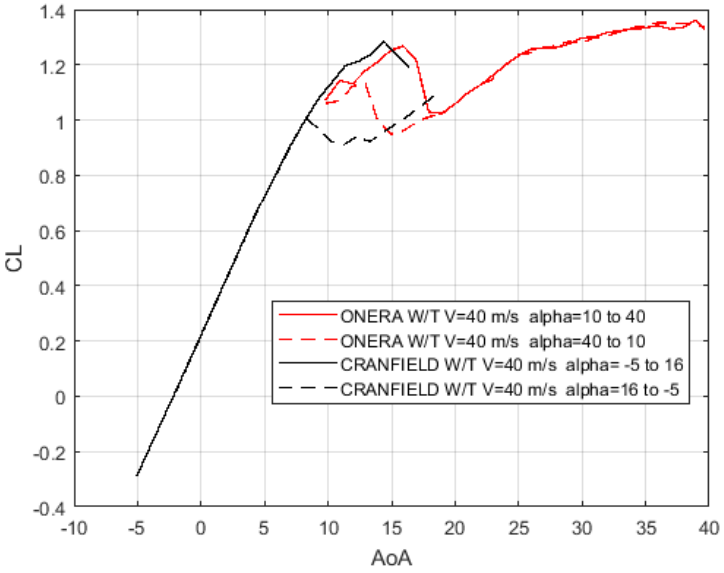


Figure 6 - Lift coefficient vs angle of attack – showing hysteresis effects from ONERA's SV4 and CRANFIELD's static W/T measurements).

3.1.3 Repeatability

Repeatability of static test has been also studied, mean values of longitudinal coefficients and standard deviations sigma have been evaluated on the set of similar tests performed at different times in the test campaign (7 tests at V=50 m/s and 12 tests at V=35 m/s) (Figure *7*). The larger deviation is observed in the stall region, corresponding to a variation of stall angle of +- 1 degree (the dotted lines refer to 1-sigma deviation). When building a model this aspect has to be taken into account for sensitivity study to model errors.

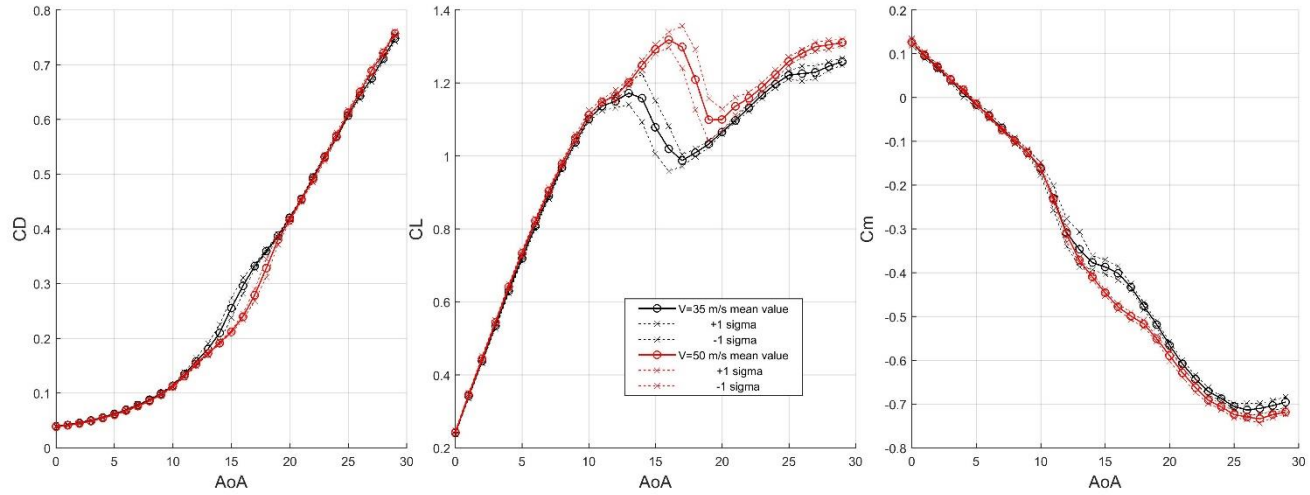


Figure 7 - Mean values and standard deviations on the set of static tests at V=35 m/s (black) and 50 m/s (red)

3.1.4 Lateral effects

Sweeps in angle of attack have been carried out at various angles of sideslip (beta=-10, -15, 0, +5, +10, +15°). As lateral stability of the aircraft especially near the stall is the main question, we will focus on the rolling and yawing moment coefficients (Figure 8). The tests put in evidence that natural stability (diheral effects) vanishes near the stall. We can remark also a natural tendancy to roll on the left side. Concerning yawing moment, yaw stability is maintained up to alpha=25°, so well beyond stall. Near the stall we remark a strong enhanced yaw stability if the sideslip remains between -10 and +10°. This behaviour does not exist at beta=+15°.

At higher angles between alpha=25 and 45° inverted effect appears (natural istability in yaw).

These results put in evidence therefore a very non-linear dependence to angles of attack and sideslip. The mathematical model is generally based on interpolation into 2-D lookup tables in order to keep all these non-linearities.

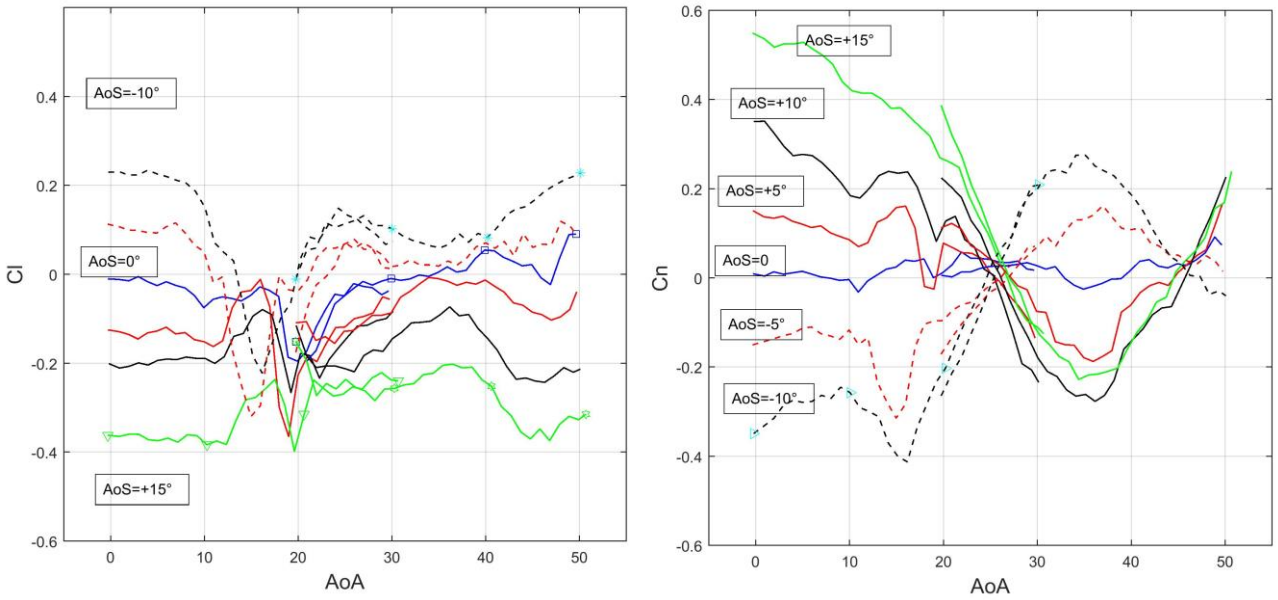


Figure 8 - Rolling and yawing moment coefficients during angle of attack sweeps [0 30°] and [20 50°] at various values of sideslip angle

3.2 Control surfaces

The model is equipped with moveable control surfaces. Extreme and medium deflections have

been tested in order to evaluate the ability to control the aircraft in a very wide domain, from normal flight to stall, and also beyond stall for recovery of incipient spin for example. Presented results are relative to quasi-static alpha_sweep tests. Efficiency of elevator is kept in a very wide range of angle of attack (*Figure 9*).

Concerning lateral control a very rapid decrease of ailerons efficiency is remarked in a range of 5° of angle of attack after stall angle (Figure 10). Another remarkable point is that ailerons are efficient again at higher angles. This is quite interesting as this is a region where rudder is almost no longer effective, due certainly to the wake of the wing (*Figure 11*).

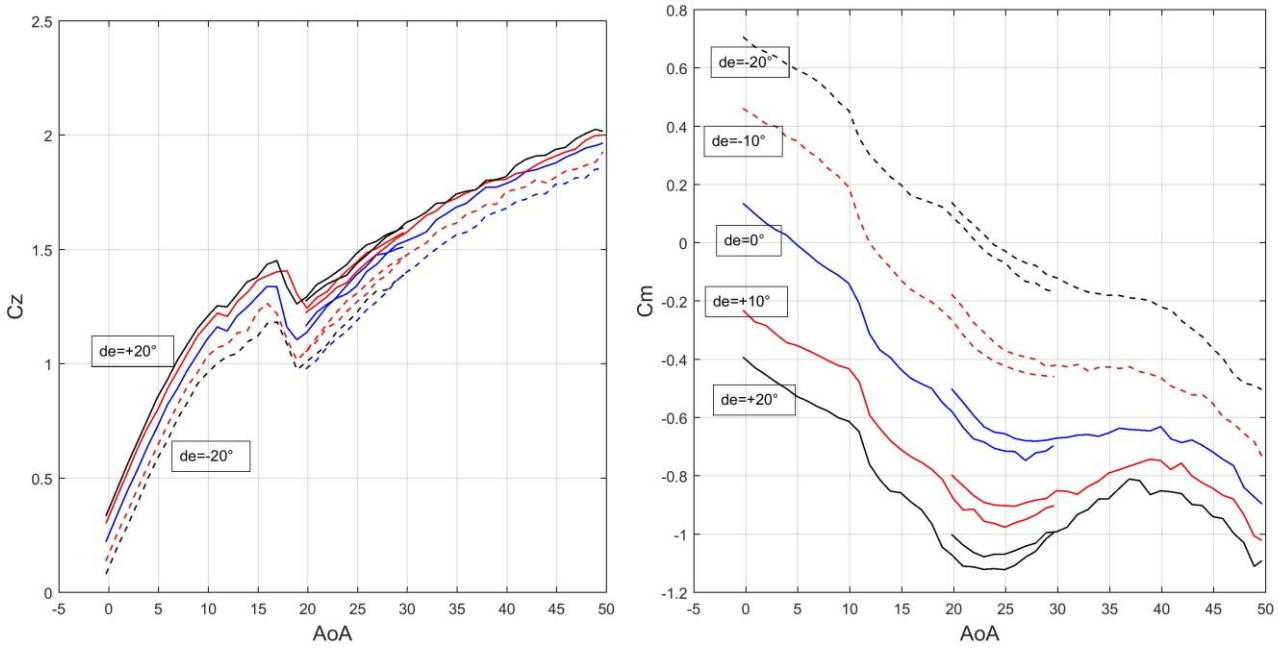


Figure 9 - Elevator deflection (de): effect on normal force and pitching moment coefficients during angle of attack sweeps [0 30°] and [20 50°]

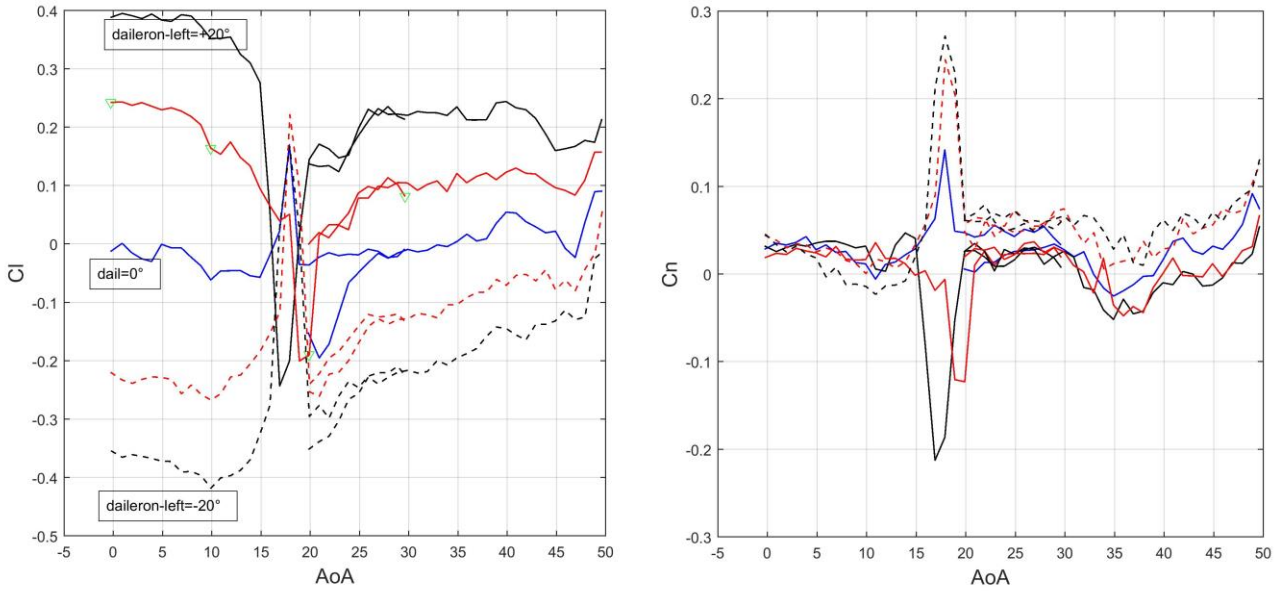


Figure 10 - Ailerons deflections: effect on rolling and yawing moment coefficients

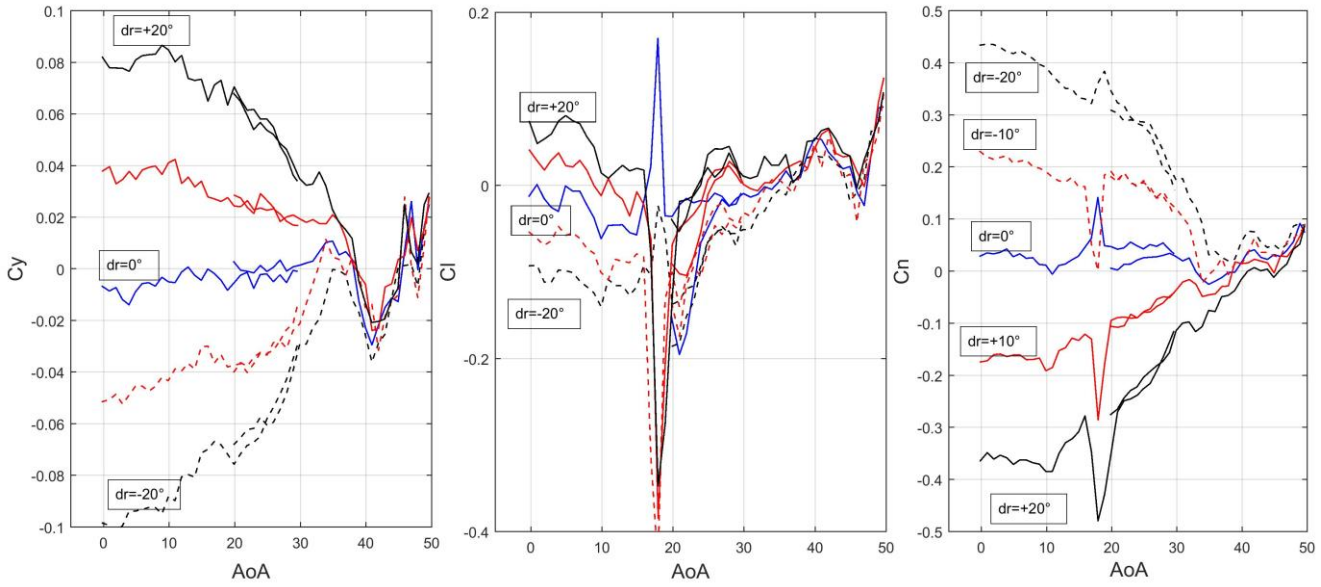


Figure 11 - Rudder deflection (dr): effect on side force, rolling and yawing moment coefficients

3.3 Coning tests

Coning motion tests allow to identify the effects of the rotation around the velocity axis. These tests are carried out at different angles of attack and sideslip, with more efforts near the stall. Inversion of roll damping occurs indeed in this range of angles and generates the phenomenon of autorotation, and therefore the departure and the entry into a spin. The autorotation is very sensitive to angles of attack and sideslip but also to controls settings.

Rolling and yawing moment coefficients are plotted versus reduced rate of rotation, which varies between -0.19 to +0.19 during a test. Coning tests are carried out at angles of attack between 0 and 40°, with a step of 5°, except between alpha=10 and 20° where cases of alpha=12.5 and 17.5° are added in order to get refined results in the vicinity of the stall (Figure 12). It should first noted that coefficients are strongly non linearly dependent to angle of attack, but also to rate of rotation.
Calculation of the slope of the rolling moment evolution relative to rate of rotation around zero value is also plotted in function of alpha (Figure 13). This put in evidence clearly two different regions: natural damping-in-roll at low angles of attack and inverted behaviour beyond alpha=12.5°, where aerodynamic effect is clearly pro-rotation, indicated by a high positive slope at alpha=15°.

The plots indicates also that a purely static aerodynamic representation based only on angle of attack and sideslip is insufficient. The results show that reduced rotation rate must be included explicitly, for example through three-dimensional lookup tables in α, β, and Ω*.. As example, we can note that at alpha=10°, variation of rolling moment with rate of rotation Is quite linear in an interval centred at Omega=0 (high damping), but at higher rates the value is stagnating. Similar behaviour (but of opposite sign) is encountered at alpha=15°.

Taking into account sideslip angle is also of great importance, as this strongly influences the tendency to the roll departure as it can be observed on Figure 14 that shows comparison between the case at beta=0 and beta=+10°. Non-coordinated flight is very often encountered in the events of loss of control, this may be due to non-adequate control settings or to the onset of cross wind. This situation is of course critical at low speeds and high angle of attack, during the landing approach where suddenly occurrence of sidewind may change the damping-in-roll.

The chosen approach for modelling is to interpolate into look-up tables, which give the values of aerodynamic coefficients in function of 3D entry (angles of attack, sideslip angle and reduced rate of rotation).

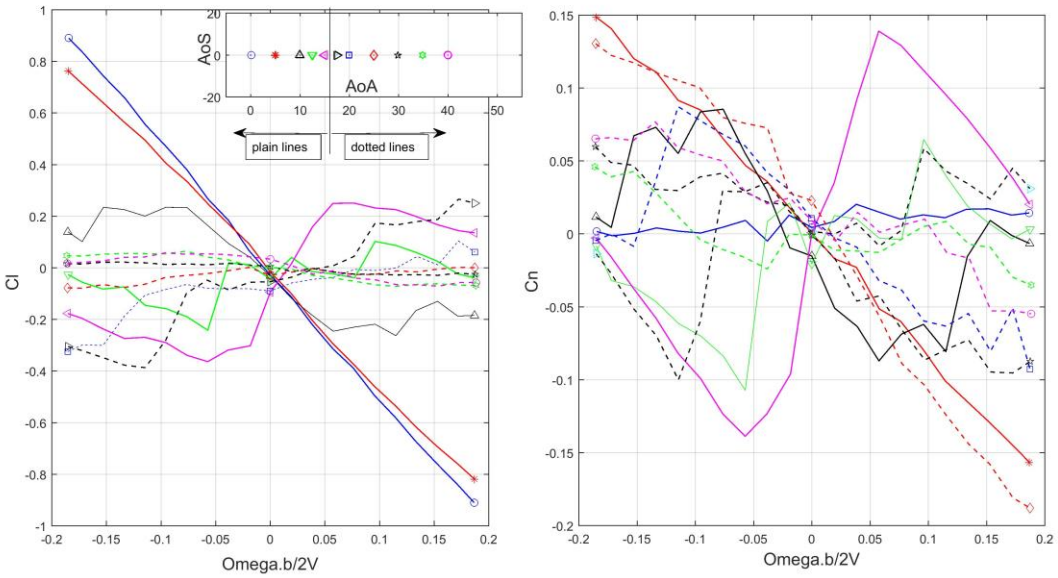


Figure 12 - Coning tests at beta=0, alpha=0, 5, 10, 12.5, 15, 17.5, 20, 25, 30, 35, 40. Rolling and yawing moments Vs reduced rate of rotation

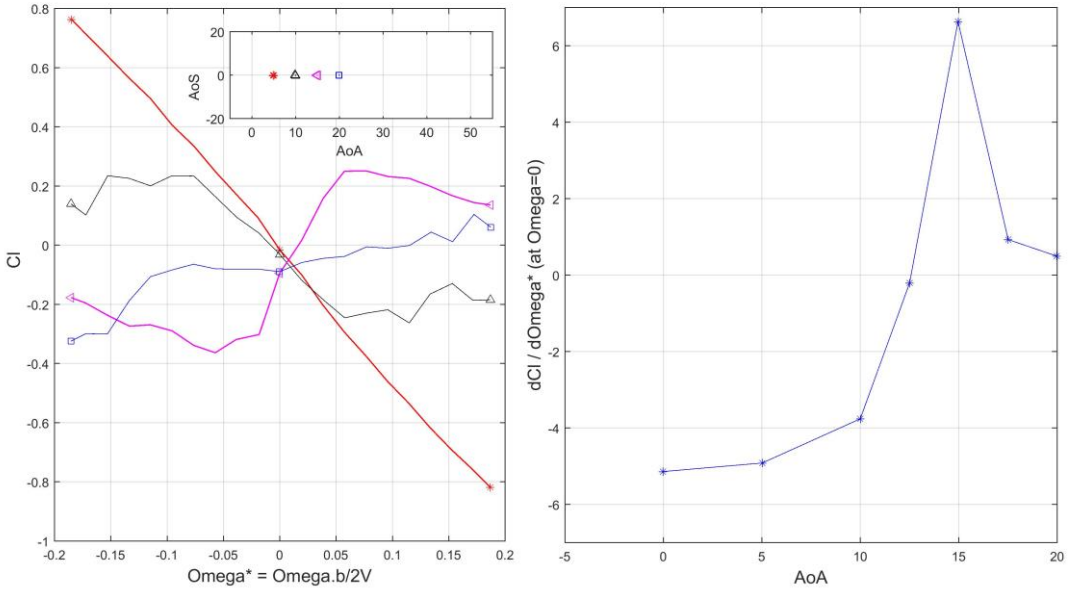


Figure 13 - Coning tests at beta=0, alpha=5, 10, 15, 20°. Rolling moment Vs reduced rate of rotation and Slope at Omega=0

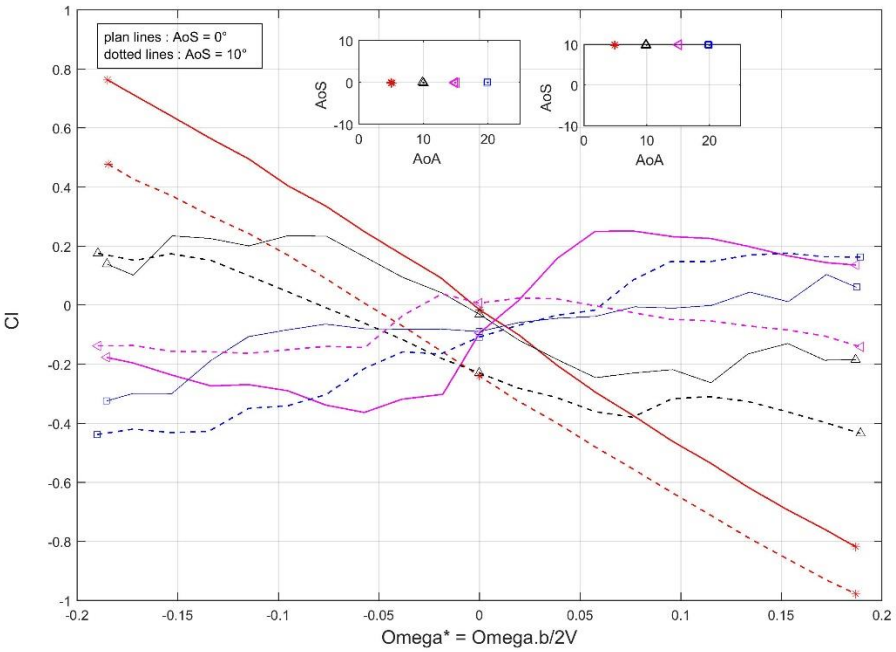


Figure 14 - Coning tests at beta=0 and +10° (dotted lines), alpha=5, 10, 15, 20°. Rolling moment Vs reduced rate of rotation

3.4 Oscillatory coning tests

Oscillatory coning tests consists in rotations about an axis which is tilted relative to wind-axis. This generates variations of angles of attack and of sideslip during a cycle. This allows therefore to capture unsteady dynamic effects if any. Evolutions of lift and pitching moment coefficient are plotted (Figure 15) when a tilt angle of 5° is considered. It can be seen that for the tests centred at alpha=5 and 10° (and therefore corresponding to rapid evolutions in [0 10°] and [5 15°] domain, the upper part of curves which is relative to increasing angle is almost aligned on static characteristics (dynamic effect is therefore very low), but in the reverse sense (decreasing angle from a high value situation) the lift coefficient appears significantly lower that for the static condition. The dynamic contribution to a given aerodynamic coefficient may be estimated by comparing the coefficient measured during a high-rate oscillatory coning test with that obtained from a slow-rate reference case following the same nominal (α, β) trajectory.

Dynamic effect is built from the difference between a test at high rotation rate (here +-500°/s) and a test at slow rate (30°/s) which gives a quasi-static reference. These terms are then considered for the mathematical model. A classical approach is to consider a first order function between dynamic part of the coefficient and the rate of variation of angle of attack.

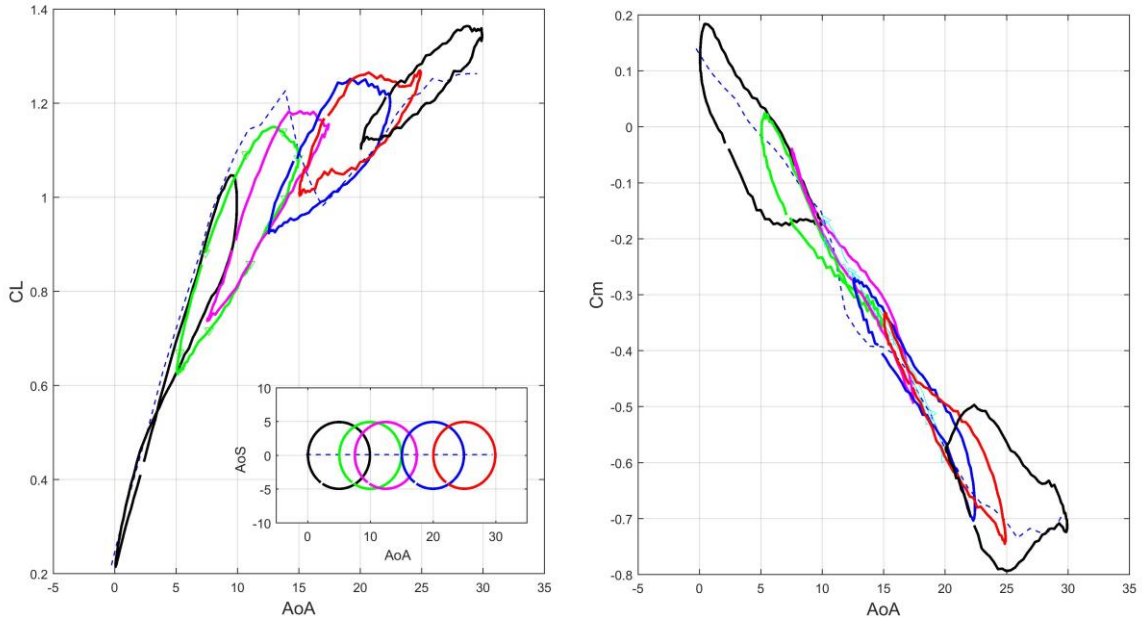


Figure 15 - Oscillatory Coning tests centered at beta=0, alpha=5, 10, 12.5, 15, 20°, 25°. Evolutions of Lift and pitching moments coefficients (Omega=500°/s V=35 m/s) (inserted : (α, β) trajectory)

The resulting lift and pitching-moment responses are shown in Figure 15 for oscillatory coning tests with a tilt angle of 5°. For the cases centred at ($\alpha = 5°$ and $\alpha = 10°$), the increasing-angle portion of the response remains close to the static characteristic, indicating limited dynamic effect during the upstroke. During the decreasing-angle portion, however, the lift coefficient is noticeably lower than the corresponding static value, suggesting a path-dependent aerodynamic response associated with separated-flow recovery.

4. Conclusions

A collaborative programme between Cranfield University and ONERA has been established on the subject of prediction of the stall and post stall behaviour of a transport aircraft. The ONERA SV4 rotary-balance campaign extends the previous Cranfield wind-tunnel tests by covering a wider range of angles of attack, sideslip angles, control-surface deflections, and rotation rates. The combined datasets provide complementary information on the static and dynamic aerodynamic characteristics of the model in nominal, stall, and post-stall conditions.

The static tests showed strong nonlinear aerodynamic behaviour near and beyond stall, including sensitivity to sideslip angle and significant changes in lateral-directional stability. The control-surface tests also demonstrated that control effectiveness can vary substantially in the post-stall regime, particularly for the lateral-directional controls. These effects highlight the limitations of aerodynamic models based only on small-disturbance or pre-stall assumptions.

Dynamic testing using coning motions enabled the identification of rate-dependent aerodynamic effects, with results showing that the rotation rate about the velocity axis plays a dominant role in governing the tendency toward stall departure. The measured aerodynamic moments exhibit strong sensitivity to angular rate, providing direct insight into the mechanisms leading to stable or unstable post-stall behaviour. The wind-tunnel tests also showed strong sensitivity to sideslip angle, confirming the need to include sideslip effects in the nonlinear aerodynamic model.

The combined experimental datasets (static and dynamic tests) are used for development of a nonlinear mathematical model of the aerodynamic characteristics, covering a wide range of angles of attack, sideslip angles, angular rates, and control-surface deflections, from nominal flight conditions to the post-stall regime. This model will provide the basis for subsequent flight-dynamic

simulation, handling-qualities assessment, and analysis of departure-prone flight conditions. Future work will also consider complementary computational-fluid-dynamics studies in the vicinity of stall, including both static and dynamic motion cases.

5. Contact Author Email Address

mailto: dominique.farcy@onera.fr

6. Copyright Statement

The authors confirm that they, and/or their company or organization, hold copyright on all of the original material included in this paper. The authors also confirm that they have obtained permission, from the copyright holder of any third party material included in this paper, to publish it as part of their paper. The authors confirm that they give permission, or have obtained permission from the copyright holder of this paper, for the publication and distribution of this paper as part of the ICAS proceedings or as individual off-prints from the proceedings.

References

[1] Whidborne, J.F., Place, S., Alam, M. and Lu, L., 2024. Supporting Flight Dynamics, Parameter Identification and Simulation Teaching with a Flying Classroom. *IFAC-PapersOnLine*, *58*(16), pp.17-22.

[2] Millidere, M., Alam, M., Place, S., Mirjalili, S., and Whidborne, J., “Aerodynamic Modelling of Saab 340B Development Using Binary Particle Swarm Optimization,” 2024. https://doi.org/10.2514/6.2024-1495

[3] Bragado-Aldana, E., Whidborne, J. F., and Alam, M., “Early-Stage Assessment of a Flexible Aircraft Simulation Framework in a Pilot-in-the-Loop Environment,” 2025. https://doi.org/10.2514/6.2025-3744

[4] Dominique Farcy, Alexander Khrabrov, Maria Sidoryuk, Sensitivity of Spin Parameters to Uncertainties of the Aerodynamic Model of a Light Aircraft. *May 2020 Journal of Aircraft 57(5):1-16 DOI: 10.2514/1.C035882*